

Article

Hysteresis-Free Piezoresponse in Thermally Strained Ferroelectric Barium Titanate Films

Marina Tyunina ^{1,2,*}, Jan Miksovsky ¹, Tomas Kocourek ¹ and Alexandr Dejneka ¹ 

¹ Institute of Physics of the Czech Academy of Sciences, Na Slovance 2, 18221 Prague, Czech Republic; miksov@fzu.cz (J.M.); kocourek@fzu.cz (T.K.); dejneka@fzu.cz (A.D.)

² Microelectronics Research Unit, University of Oulu, P.O. Box 4500, FI-90014 Oulu, Finland

* Correspondence: tjunina@fzu.cz

Abstract: Modern technology asks for thin films of sustainable piezoelectrics, whereas electro-mechanical properties of such films are poorly explored and controlled. Here, dynamic and quasi-static polarization, dielectric, and piezoelectric responses were experimentally studied in thin-film stacks of barium titanate sandwiched between electrodes and grown on top of strontium titanate substrate. Accurate piezoelectric characterization was secured by using double beam interferometric technique. All out-of-plane responses were found to be hysteresis-free. Effective piezoelectric coefficient ~ 50 pm/V and linear strain-voltage characteristic were achieved. The observed behavior was ascribed to field induced out-of-plane polarization, whereas spontaneous polarization is in-plane due to in-plane tensile thermal strain. Hysteresis-free linear piezoresponse was anticipated in thin films on commercial silicon substrates, enabling large thermal strain.

Keywords: barium titanate; piezoelectric; ferroelectric



Citation: Tyunina, M.; Miksovsky, J.; Kocourek, T.; Dejneka, A. Hysteresis-Free Piezoresponse in Thermally Strained Ferroelectric Barium Titanate Films. *Electron. Mater.* **2021**, *2*, 17–23. <https://doi.org/10.3390/electronicmat2010002>

Received: 2 December 2020

Accepted: 12 January 2021

Published: 14 January 2021

Publisher's Note: MDPI stays neutral with regard to jurisdictional claims in published maps and institutional affiliations.



Copyright: © 2021 by the authors. Licensee MDPI, Basel, Switzerland. This article is an open access article distributed under the terms and conditions of the Creative Commons Attribution (CC BY) license (<https://creativecommons.org/licenses/by/4.0/>).

1. Introduction

Perovskite oxide ferroelectrics are known to exhibit excellent electro-mechanical properties that makes these materials major piezoelectrics [1,2]. Numerous piezoelectric applications of ferroelectric ceramics and crystals are commercialized and being continuously developed. Beyond this mainstream technology, modern sustainability requirements as well as demands for micro- and nanoscale devices stimulate advancement of piezoelectric thin films, which are free of hazardous elements such as lead and niobium [3] and only a few to less than one micron in thickness. Moreover, for many applications it is crucial that piezoelectric strain-electric field behavior is free of hysteresis. Such hysteresis is typical for ferroelectrics and originates from the presence of domains with different orientations of spontaneous polarization. A certain coercive field is required to switch polarization, that leads to polarization—electric field hysteresis. Consequently, the dielectric permittivity and piezoelectric coefficient exhibit hysteresis in their field-dependent behavior.

It is worth noting that compared to ceramics, domain configuration of thin films strongly depends on elastic coupling between a film and an underlying substrate. For a vertical stack of a tetragonal ferroelectric film sandwiched between electrodes (metal layers) and grown on top of a crystal substrate (Figure 1a), there are two limiting cases of domains: *c*-type domains, where polarization direction is aligned normal to the substrate surface, or in the out-of-plane direction (Figure 1b), and *a*-type domains, where polarization direction is aligned parallel to the substrate surface, or in the in-plane direction (Figure 1c). For many ferroelectric materials, piezoelectric out-of-plane deformation is larger in the *c*-type films than in the *a*-type ones when electric field is applied in the out-of-plane direction (Figure 1a). Whereas epitaxial *c*-type films allow for maximizing piezoresponse magnitude, switching of the 180° *c*-domains produces strong hysteresis therein. The presence of *a*-type domains diminishes coercive field (voltage) at the expense of response magnitude.

Therefore, engineering domain configuration is one of the tools for tailoring piezoelectric properties of thin films.

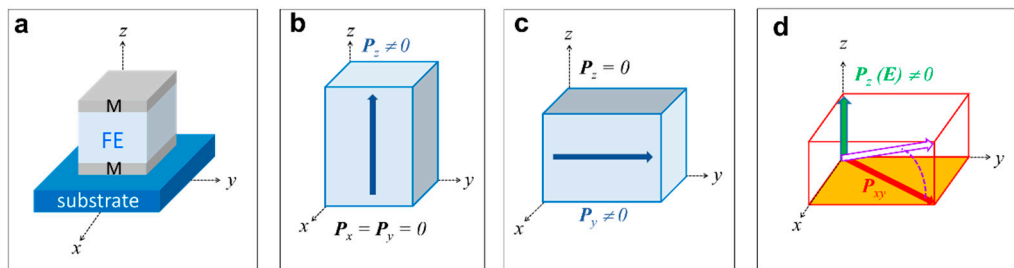


Figure 1. Schematics of (a) thin-film ferroelectric metal-ferroelectric-metal stack, (b) c-domain with out-of-plane polarization, (c) a-domain with in-plane polarization, (d) exaggerated r-type domain with spontaneous in-plane polarization and electric-field induced out-of-plane polarization.

In recent decades, control of domain configuration was extensively studied in epitaxial ferroelectric films. By using a substrate, whose lattice parameters are smaller than those of a ferroelectric material, a biaxial in-plane compressive misfit strain can be imposed on the film and stimulate the formation of *c*-domains therein. Correspondingly, to enforce in-plane polarization, a tensile substrate should be employed. The type, width, and spatial distribution of different domains result from a delicate interplay between misfit strain, thickness of the film, and properties of the film's material [4]. Practical implementation of this fascinating approach is, unfortunately, restricted by selection of appropriate substrates, which may be too expensive, difficult to synthesize, or unavailable in reality.

Here, we demonstrate that, instead of the film-substrate lattice misfit, a film-substrate mismatch in the coefficients of thermal expansion (CTE) can be effectively used to manage domains and achieve hysteresis-free piezoresponse. Synthesis of perovskite-structure ferroelectric films requires high temperatures of 800–1200 K. During cooling from the synthesis (deposition) temperature, the CTE mismatch causes a build-up of a thermal strain in the films. The linear CTE values are positive and typically $(0.6\text{--}1.5) \times 10^{-5} \text{ K}^{-1}$ in the high-temperature cubic paraelectric phase of many ferroelectrics, about $(0.7\text{--}1.3) \times 10^{-5} \text{ K}^{-1}$ in common oxide substrates, and as small as $0.26 \times 10^{-5} \text{ K}^{-1}$ at 300 K and $4.2 \times 10^{-5} \text{ K}^{-1}$ at 1000 K in silicon, which is the main commercial substrate material [5–10]. These coefficients ensure possibility for tensile thermal-mismatch strain (or thermal strain here for brevity) in ferroelectric films. Moreover, this strain can be continuously varied by altering deposition temperature [11].

Here we focus on archetypical, environmentally friendly, biocompatible, and low-cost ferroelectric BaTiO₃ (BTO), which is a basis for sustainable piezoelectrics [12]. To enable epitaxial growth and thermal tension, we employed research SrTiO₃ (STO) substrates. The BTO/STO compressive misfit strain is large and relaxes during deposition, whereas tensile thermal strain builds up on cooling [13,14]. The thermal tension produces an *r*-type phase, where spontaneous polarization is in-plane and where an out-of-plane polarization can be induced by the application of out-of-plane electric field. The total polarization rotates toward the out-of-plane direction (Figure 1d). Using this mechanism, nearly hysteresis-free polarization was previously achieved in 200–400 nm thick films [13]. Here we report on hysteresis-free piezoresponse in the thermally strained BTO films with thickness of $\sim 1 \mu\text{m}$. The films possess effective piezoelectric coefficient to $\sim 50 \text{ pm/V}$ and exhibit linear strain-field behavior. We anticipate that the demonstrated effect can be valid also for thin films grown on commercial silicon substrates.

2. Materials and Methods

Thin films of BTO and SrRuO₃ (SRO) bottom electrode were grown by pulsed laser deposition (PLD) using a KrF excimer laser (energy density $\sim 2 \text{ J/cm}^2$) at a substrate temperature of 973 K and a pressure of ambient oxygen of 20 Pa. Postdeposition cooling was

conducted at a rate of 5 K/min. Epitaxially polished (001) STO substrates were purchased from MTI Corporation. The thickness of the films was controlled by number of laser pulses and measured on a KLA-Tencor Alpha-Step IQ Surface Profilometer (KLA Instruments, Milpitas, CA, USA) using a step, which was formed by shadow masking during PLD. Concurrently, the surface roughness of the films was inspected using this Profilometer. The crystal structure of the films was characterized by X-ray diffraction on D8 DISCOVER diffractometers (Bruker corporation, Berlin, Germany) using Cu K α radiation. More details on structural and morphological characterization can be found elsewhere [13,14]. Cube-on-cube growth and in-plane tensile strain in BTO were confirmed by θ - 2θ scans and reciprocal space mapping (Supplementary Figure S1).

For electrical and piezoelectric characterization, capacitor stacks were formed using circular top Pt contact pads (diameter 2 mm), created by room-temperature vacuum PLD of Pt through a shadow mask. To ensure high accuracy of double beam interferometric measurements of piezoresponse, the thickness of the optically reflecting top Pt electrodes was 60 nm. Back sides of the substrates were polished, and a highly reflecting Au layer was deposited thereon by PLD and sputtering. To safeguard reliable adhesion and stability of the backside reflecting layer, a thin PLD-prepared layer of Au was introduced prior to sputtering.

The quasi-static and dynamic polarization–voltage loops, leakage current, dynamic out-of-plane elongation–voltage loops, capacitance–bias curves, and effective piezoelectric coefficient–bias curves were measured on a double beam laser interferometer DBLI (aixACCT Systems GmbH, Aachen, Germany) equipped with a TF 2000 E Analyzer (aixACCT Systems GmbH, Aachen, Germany). For the measurements of capacitance and effective piezoelectric coefficient, the biasing dc voltage was superimposed with small ac voltage and swept from zero to a maximum positive, maximum negative, and back to zero voltages. In all measurements, the electric field was applied and the responses were acquired in the out-of-plane direction.

3. Results and Discussion

It was shown before that thermal tension enforces polarization to stay in-plane (Figure 1d) in the BTO films on STO [13,14]. Such a phase was predicted theoretically and is characterized by the two in-plane polarization components being non-zero [15–17]. The out-of-plane spontaneous polarization is zero, and the out-of-plane polarization–voltage curve is expected to be linear. However, the applied electric field induces a non-zero out-plane polarization component and thus causes a transformation to another, *r*-type phase, which was also predicted theoretically. The total polarization rotates out from the in-plane location under the applied field (Figure 1d) and turns back when the field is switched off. Correspondingly, the measured quasi-static polarization–voltage curve is not linear. Because polarization rotations are nearly instantaneous, there is no remnant polarization. The hysteresis-free quasi-static polarization–voltage loop was obtained previously and is perfectly reproduced here (Figure 2a).

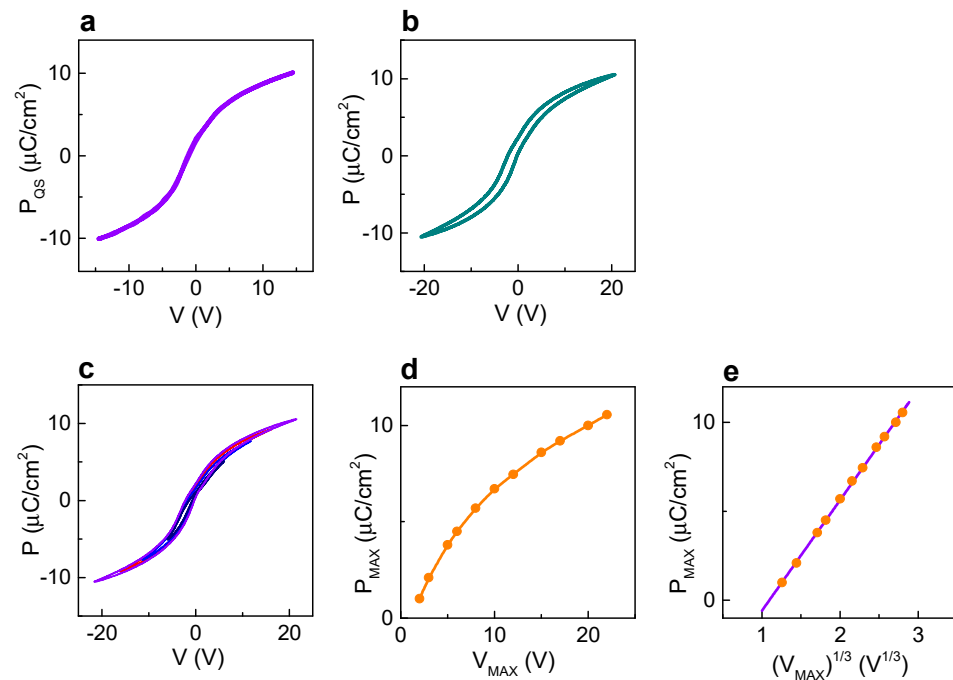


Figure 2. (a) Quasi-static polarization–voltage loop, (b,c) dynamic polarization–voltage loops at frequency 1 kHz, (d,e) maximum polarization as a function of (d) maximum voltage V_{MAX} and (e) $(V_{MAX})^{1/3}$. Straight line shows fit in (e).

Consistent with this behavior, also the dynamic polarization–voltage (P–V) loop is very slim and practically hysteresis-free (Figure 2b). We note that slim P–V loops are measured at all magnitudes of maximum applied voltage V_{MAX} (Figure 2c and Supplementary Figures S2 and S3), that is in striking contrast to regular ferroelectric loops with the Rayleigh-type shape at small sub-switching voltages. The maximum polarization P_{MAX} increases with increasing maximum voltage V_{MAX} (Figure 2c,d). The scaling behavior ($P_{MAX} \propto (V_{MAX})^{1/3}$) is evidenced by a good linear fit in Figure 2e. This polarization–voltage scaling also agrees with our previous observations of polarization rotation [13].

From the hysteresis-free polarization behavior (Figure 2), it is easy to understand the lack of hysteresis in the voltage dependence of the out-of-plane elongation Δl (Figure 3a). Remarkably, the strain–voltage characteristic is perfectly linear (Figure 3b), which is often desirable but seldom achievable.

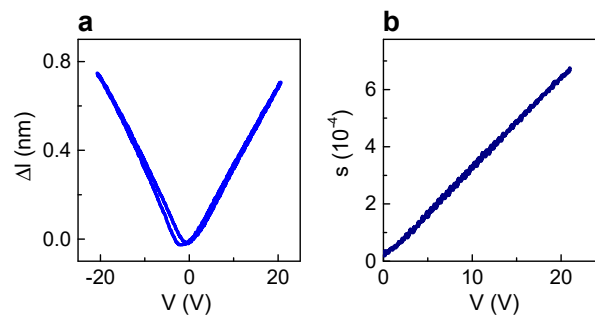


Figure 3. (a) Dynamic elongation–voltage loop at frequency 1 kHz and (b) unipolar dynamic strain.

We note that dynamic characteristics (Figures 2 and 3) are measured by applying a sine voltage of a certain amplitude, which can significantly exceed coercive voltage. Such measurements are impossible for bulk samples and, strictly speaking, their results cannot be immediately apprehended from the common point of view. Another, more conventional approach is to use a small ac voltage and superimpose a biasing dc voltage. For convenience, we denote this regime as “static” here. The real part of the dielectric permittivity, ϵ ,

and the effective piezoelectric coefficient, d^* , which were measured in the static regime, are presented in Figure 4a,b, correspondingly. Only minor hysteresis is observed for different directions of the bias sweeps in the (ϵ – V) behavior (Figure 4a), consistent with the slim dynamic (P– V) loops (Figure 2b). Correspondingly, also hysteresis in the (d^* – V) behavior is minute. To relate the results obtained in the two different regimes, the dynamic effective coefficient d^* was extracted by differentiating the strain–voltage data (Figure 3a). There is a perfect agreement between the extracted dynamic coefficient and the static one (Figure 4c).

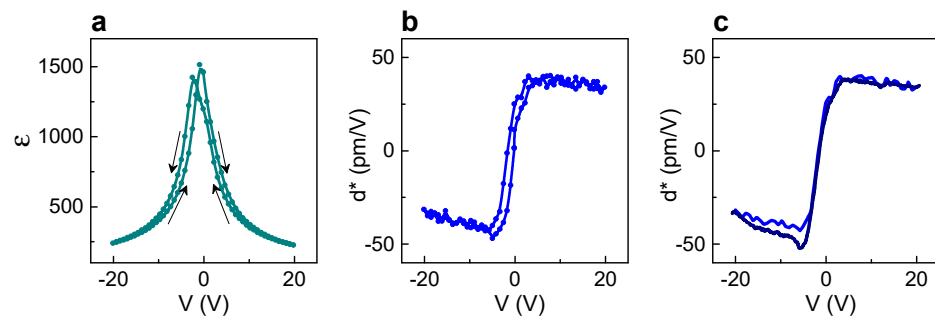


Figure 4. (a) The real part of the dielectric permittivity and (b) the static effective piezoelectric coefficient as a function of dc bias voltage (ac voltage at 1 kHz). (c) The static and the dynamic piezoelectric coefficients as a function of voltage for the ascending voltages (from -20 V to $+20$ V).

The maximum achieved magnitude of d^* is 50 pm/V, which coincides with the results of the truly static measurements using x-ray diffraction analysis [18]. It is worth emphasizing that piezoelectric coefficients reported for thin films are usually determined from dynamic responses of thin-film devices, or using piezoresponse force microscopy (PFM), or using single-beam interferometry. These methods are not free from significant uncertainties related to device modeling, PFM calibration, or substrate contribution. Here, the double-beam interferometry in combination with the specially prepared optically reflecting layers of the top surfaces of the films and on the back-side surfaces of the substrates ensured high accuracy for the effective piezoelectric coefficient.

To get a further insight into the observed nearly linear and hysteresis-free piezoelectric behavior, we calculated the polarization and the piezoelectric coefficient using the measured dielectric permittivity. For the ascending voltage branch of the (ϵ – V) sweep (Figures 4a and 5a), the polarization–voltage curve was obtained by integration as $P = \epsilon_0 \int \epsilon(V) dV$ (Figure 5b). Here, ϵ_0 is the permittivity of vacuum. The piezoelectric coefficient was then estimated as $d^* = 2Q \epsilon_0 \epsilon P$, where $Q = 0.1$ m²/C² is the coefficient of electrostriction of BTO [19]. The calculated piezoelectric coefficient is in excellent agreement with the measured ones (Figure 5c).

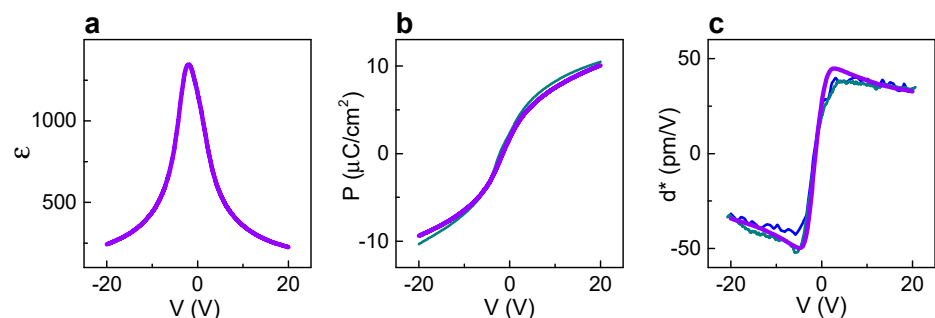


Figure 5. (a) The measured dielectric permittivity and the (b) polarization and (c) effective piezoelectric coefficient calculated from the permittivity. Thin curves show measurement results in (b,c).

The obtained direct dielectric–piezoelectric link implies a negligible, if any, role of spontaneous polarization in the out-of-plane piezoresponse. This behavior is very unusual,

but comprehensible from the field-induced polarization as illustrated in Figure 1d. We note that the *r*-type phase in the film cannot be straightforwardly compared with any of the phases in bulk BTO (i.e., tetragonal, orthorhombic, and rhombohedral). Therefore, the achieved large permittivity and piezoelectric coefficient cannot be assigned and indexed in accordance with common BTO notations. An appropriate theoretical thermodynamic potential should be developed for predictive theoretical modeling of piezoelectric behavior in the *r*-films. Finally, it is worth mentioning that the CTE mismatch between BTO and Si is very large. This mismatch suggests that profound thermally induced tensile strain can be created and used to tailor hysteresis-free and linear piezoresponse in BTO films on commercial substrates.

4. Conclusions

Polarization, dielectric permittivity, and piezoelectric response were experimentally investigated as a function of applied voltage under dynamic and quasi-static conditions in thin-film stack of archetypical, environmentally friendly, biocompatible, and low-cost ferroelectric BaTiO₃, sandwiched between electrodes and grown on top of SrTiO₃ substrate. High accuracy of piezoelectric characterization was ensured by double beam interferometric technique.

The measured out-of-plane quasi-static response functions were found to be free of hysteresis, and only a minute hysteresis was observed in the dynamic responses. The static and dynamic effective piezoelectric coefficients agreed with each other and amounted to ~50 pm/V. Concurrently, the strain-field dependence was found to be linear. A direct link between the dielectric permittivity and piezoelectric coefficient was established, discarding spontaneous polarization as contributing to the out-of-plane piezoresponse. The observations were consistent with the out-of-plane field induced polarization, whereas spontaneous polarization was in-plane due to in-plane tensile thermal strain. It was anticipated that hysteresis-free linear piezoresponse can be achieved in thin films on commercial silicon substrates, which enable large thermal strain.

Supplementary Materials: The following are available online at <https://www.mdpi.com/2673-3978/2/1/2/s1>, Figure S1: X-ray diffraction analysis, Figure S2: Dynamic polarization as a function of voltage, Figure S3: Dynamic polarization as a function of frequency.

Author Contributions: Conceptualization, investigation, methodology, writing, supervision M.T., investigation J.M. and T.K.; administration, funding acquisition M.T. and A.D. All authors have read and agreed to the published version of the manuscript.

Funding: This research was supported in part by the Czech Science Foundation (Grant No. 19-09671S) and the European Structural and Investment Funds and the Ministry of Education, Youth and Sports of the Czech Republic through Programme “Research, Development and Education” (Project No. SOLID21—CZ.02.1.01/0.0/0.0/16_019/0000760).

Institutional Review Board Statement: Not applicable.

Informed Consent Statement: Not applicable.

Data Availability Statement: The data presented in this study are available in this article and supplementary material here.

Conflicts of Interest: The authors declare no conflict of interest. The funders had no role in the design of the study; in the collection, analyses, or interpretation of data; in the writing of the manuscript, or in the decision to publish the results.

References

1. Lines, M.E.; Glass, A.M. *Principles and Applications of Ferroelectrics and Related Materials*; Clarendon Press: Oxford, UK, 2004.
2. Uchino, K. *Ferroelectric Devices*; Marcel Dekker: New York, NY, USA, 2000.
3. Ibn-Mohammed, T.; Koh, S.C.L.; Reaney, I.M.; Acquaye, A.; Wang, D.; Taylor, S.; Genovese, A. Integrated hybrid life cycle assessment and supply-chain environmental profile evaluations of leadbased (lead zirconate titanate) versus lead-free (potassium sodium niobate) piezoelectric ceramics. *Energy Environ. Sci.* **2016**, *9*, 3495–3520. [[CrossRef](#)]

4. Tagantsev, A.K.; Cross, L.E.; Fousek, J. *Domains in Ferroic Crystals and Thin Films*; Springer: New York, NY, USA, 2010.
5. Radhika Rao, M.V.; Umarji, A.M. Thermal expansion studies on ferroelectric materials. *Bull. Mater. Sci.* **1997**, *20*, 1023. [[CrossRef](#)]
6. Malic, B.; Razpotnik, H.; Koruza, J.; Kokalj, S.; Cilensek, J.; Kosec, M. Linear Thermal Expansion of Lead-Free Piezoelectric $\text{K}_{0.5}\text{Na}_{0.5}\text{NbO}_3$ Ceramics in a Wide Temperature Range. *J. Am. Ceram. Soc.* **2011**, *94*, 2275. [[CrossRef](#)]
7. de Ligny, D.; Richet, P. High-temperature heat capacity and thermal expansion of SrTiO_3 and SrZrO_3 perovskites. *Phys. Rev. B* **1996**, *53*, 3013. [[CrossRef](#)]
8. Hellwege, K.H.; Hellwege, A.M. (Eds.) *Landolt-Börnstein, Numerical Data and Functional Relationships in Science and Technology, New Series, Group III, Crystal and Solid State Physics*; Springer: Berlin, Germany, 1981.
9. Zhu, J.; Zhang, J.; Xu, H.; Vogel, S.C.; Jin, C.; Frantti, J.; Zhao, Y. Pressure-induced reversal between thermal contraction and expansion in ferroelectric PbTiO_3 . *Sci. Rep.* **2014**, *4*, 3700. [[CrossRef](#)] [[PubMed](#)]
10. Biegalski, M.D.; Haeni, J.H.; Trolier-McKinstry, S.; Schlom, D.G.; Brandle, C.D.; Ven Graitis, A.J. Thermal expansion of the new perovskite substrates DyScO_3 and GdScO_3 . *J. Mater. Res.* **2005**, *20*, 952. [[CrossRef](#)]
11. Zhang, L.; Yuan, Y.; Lapano, J.; Brahlek, M.; Lei, S.; Kabius, B.; Gopalan, V.; Engel-Herbert, R. Continuously Tuning Epitaxial Strains by Thermal Mismatch. *ACS Nano* **2018**, *12*, 1306. [[CrossRef](#)] [[PubMed](#)]
12. Acosta, M.; Novak, N.; Rojas, V.; Patel, S.; Vaish, R.; Koruza, J.; Rossetti, G.A.; Rödel, J. BaTiO_3 -based piezoelectrics: Fundamentals, current status, and perspectives. *Appl. Phys. Rev.* **2017**, *4*, 041305. [[CrossRef](#)]
13. Tyunina, M.; Pacheroova, O.; Peräntie, J.; Savinov, M.; Jelinek, M.; Jantunen, H.; Dejneka, A. Perovskite ferroelectric tuned by thermal strain. *Sci. Rep.* **2019**, *9*, 3677. [[CrossRef](#)] [[PubMed](#)]
14. Tyunina, M.; Peräntie, J.; Kocourek, T.; Saukko, S.; Jantunen, H.; Jelinek, M.; Dejneka, A. Oxygen vacancy dipoles in strained epitaxial BaTiO_3 films. *Phys. Rev. Res.* **2020**, *2*, 023056. [[CrossRef](#)]
15. Shirokov, V.B.; Yuzyuk, Y.I.; Dkhil, B.; Lemanov, V.V. Phenomenological theory of phase transitions in epitaxial BaTiO_3 thin films. *Phys. Rev. B* **2007**, *75*, 224116. [[CrossRef](#)]
16. Shirokov, V.B.; Yuzyuk, Y.I.; Dkhil, B.; Lemanov, V.V. Phenomenological Description of Phase Transitions in Thin BaTiO_3 Films. *Phys. Solid State* **2008**, *50*, 928. [[CrossRef](#)]
17. Dieguez, O.; Tinte, S.; Antons, A.; Bungaro, C.; Neaton, J.B.; Rabe, K.M.; Vanderbilt, D. Ab initio study of the phase diagram of epitaxial BaTiO_3 . *Phys. Rev. B* **2004**, *69*, 212101. [[CrossRef](#)]
18. Thery, V.; Bayart, A.; Blach, J.F.; Roussel, P.; Saitzek, S. Effective piezoelectric coefficient measurement of BaTiO_3 thin films using the X-ray diffraction technique under electric field available in a standard laboratory. *Appl. Surf. Sci.* **2015**, *351*, 480–486. [[CrossRef](#)]
19. Lia, Y.L.; Cross, L.E.; Chen, L.Q. A phenomenological thermodynamic potential for BaTiO_3 single crystals. *J. Appl. Phys.* **2005**, *98*, 064101. [[CrossRef](#)]